European Journal of Pharmaceutics and Biopharmaceutics 136 (2019) 138–146

Contents lists available at ScienceDirect

European Journal of Pharmaceutics and Biopharmaceutics

journal homepage: www.elsevier.com/locate/ejpb

Research paper

Efficacy of a novel LyP-1-containing self-microemulsifying drug delivery system (SMEDDS) for active targeting to breast cancer

Selin S. Timur[a], Diğdem Yöyen-Ermiş[b,1], Güldal Esendağlı[c], Selcen Yonat[c], Utku Horzum[b], Güneş Esendağlı[b], R. Neslihan Gürsoy[a,*]

[a] Department of Pharmaceutical Technology, Faculty of Pharmacy, Hacettepe University, Ankara, Turkey
[b] Department of Basic Oncology, Hacettepe University Cancer Institute, Ankara, Turkey
[c] Department of Medical Pathology, Faculty of Medicine, Gazi University, Ankara, Turkey

ARTICLE INFO

Keywords:
Breast cancer
LyP-1
p32
SMEDDS
Lymphatic targeting
Chemotherapy

ABSTRACT

An ideal cancer therapy targets the tumor cells selectively without damaging healthy tissues. Even though the tumor-specific markers are limited, these molecules can be used for the delivery of anti-cancer drugs as an active targeting strategy. Since the lymphatic system plays a critical role in the dissemination of cancer cells, the drugs directed through lymphatics can feasibly reach to the sites of metastasis. LyP-1 is a peptide that binds to the p32 receptor which is highly expressed not only on the lymphatic endothelium but also on the malignant cells; thus, making this peptide ligand a preferable candidate to mediate active targeting of lymphatics and cancer cells. In this study, different formulations of LyP-1 containing lipid-based nanopharmaceutics so-called self-microemulsifying drug delivery systems (SMEDDS) were developed and tested for their efficacy in targeting breast cancer. Following the selection of non-toxic formulation, doxorubicin hydrochloride and LyP-1 were co-administered in the SMEDDS, which resulted in a significant increase in in vitro cytotoxicity in p32-expressing breast cancer cells, 4T1 and MDA-MB-231. Accordingly, the uptake of LyP-1 in the SMEDDS by the cancer cells was demonstrated. The expression of p32 was detected in the 4T1 tumor tissues which were efficiently targeted with LyP-1 in the SMEDDS. When doxorubicin was co-administrated with LyP-1 in SMEDDS via intraperitonial administration, tumor growth and metastasis were significantly reduced. In conclusion, a novel and efficacious SMEDDS formulation containing LyP-1 with a droplet size less than 100 nm was developed for the lymphatic targeting of breast cancer.

1. Introduction

The real challenge of conventional anticancer therapy is to overcome the undesirable collateral damage on healthy tissues, especially with high renewal capacity [1]. Thus, studies that adopted a passive or active therapy approach aim to selectively and effectively deliver the drugs into the tumor [2]. The receptors on the surface of tumor cells can be targeted by the drug delivery systems bearing specific ligands. These approaches not only enable the delivery of low dose chemotherapeutics but also ensure the effectiveness [3].

The lymphatic system plays crucial roles in homeostasis, lipid absorption and immune response, albeit serving as a path for the metastatic spread of cancer cells [4]. Thus, lymphatics has become a preferable target for anti-cancer drug delivery systems [5–8]. LyP-1 is a nonapeptide (CGNKRTRGC) with an ability to bind its specific receptor p32 (gC1qR/HABP), which can be highly found on tumor-related lymphatics, macrophages, and cancer cells [9,10]. Elevated levels of p32 is found on the surface of cancer cells while it is intracellularly expressed in normal cells; therefore, p32 found on cancer cells and lymphatic endothelium is more accessible by LyP-1 [9,11–13].

In addition to its tumor homing abilities, LyP-1 can deteriorate the viability of MDA-MB-435 breast cancer cells in a dose-dependent manner. Repeated administration of LyP-1 was shown to hamper the tumor progression and the development of new lymphatics in the tumors established with MDA-MB-435 [10]. Accordingly, LyP-1 has become a preferred molecule for the active targeting of cancer and lymphatics in cancer diagnosis and treatment studies. This peptide has been used in formulations prepared with liposomes [14–17], dendrimers [18,19], microbubbles [20–22], SMEDDS [23], micelles [24,25], nanoparticles [11,26–32], and mesoporous nanospheres [33].

* Corresponding author.
E-mail address: ngursoy@hacettepe.edu.tr (R.N. Gürsoy).
[1] Current address: Medical Biology Department, Faculty of Medicine, Lokman Hekim University, Ankara, Turkey.

https://doi.org/10.1016/j.ejpb.2019.01.017
Received 13 September 2018; Received in revised form 2 January 2019; Accepted 16 January 2019
Available online 22 January 2019
0939-6411/

The self-emulsifying drug delivery systems (SEDDS) are isotropic systems which consist of oil, surfactant and cosurfactant/cosolvent mixtures and form thermodynamically stable micro/nanoemulsions by gentle agitation upon dilution with aqueous media [23,34–44]. The droplet size of SEDDS is defined between 100 and 300 nm, while self-microemulsifying drug delivery systems (SMEDDS) form stable microemulsions with droplets less than 100 nm [34,45]. The SEDDS are commonly developed for the oral administration of peptide/protein drugs and poorly water-soluble drugs. The permeation enhancer effect and protection against lipases are the advantages of these systems [46]. The SEDDS can also enable parenteral and oral administration of cancer therapeutics such as paclitaxel [47–49], docetaxel [50] and erlotinib [51].

In this study, the SMEDDS formulations harboring LyP-1 peptide were developed for selective targeting of lymphatics and breast tumors. The therapeutic efficacy of the system alone or in combination with doxorubicin hydrochloride (Dox HCl) was evaluated in vitro on p32-expressing breast cancer cells and in vivo on tumor-bearing mice. Here, we report a novel and efficacious formulation of LyP-1-containing SMEDDS with a droplet size less than 100 nm for the targeting of chemotherapeutics into breast tumors.

2. Materials and methods

2.1. Materials

Cyclic LyP-1 and LyP-1-FAM peptides were purchased from Innovagen AB (Sweden). Labrasol®, Maisine™, Peceol™ and Gelucire® 44/14 were kind gifts from Gattefossé (Lyon, France) and kindly provided by KURA Chemical Products Trade Inc. Co. (Istanbul, Turkey). All other chemicals were analytical grade, unless otherwise stated.

2.2. Preparation and characterization of SMEDDS formulations

Preformulation studies were performed utilizing ternary phase diagrams to select the optimum excipients to obtain self-emulsification with droplet size under 100 nm for lymphatic targeting. Caprylocaproyl polyoxyl-8 glycerides (Labrasol®), lauroyl polyoxyl-32 glycerides (Gelucire® 44/14), oleoyl polyoxyl-6 glycerides (Labrafil® M1944 CS), D-[alpha]-tocopheryl polyethylene glycol succinate (TPGS) and polysorbate 80 (Tween® 80) were used as surfactants; glyceryl monooleate (Type 40) (Peceol™), glyceryl monolinoleate (Maisine™ 35-1), soybean oil, sunflower oil and alpha tocopherol as the oil phase and polyethylene glycol 300, propylene glycol and diethylene glycol monoethyl ether (Transcutol® HP) as cosolvents to determine the optimum formulation components for the SMEDDS. All the excipients selected were pharmaceutical grade and suitable for both oral and parenteral administration. For the selection of the oil phase, the excipients were evaluated in the order of increasing lymphatic uptake of the prepared formulations [36,52,53]. All prepared formulations were evaluated in terms of physical stability, droplet size distribution and liquid crystal formation. For the preparation of blank liquid SMEDDS formulations (without peptide and/or Dox HCl); the oil phase, surfactant and cosolvents were simply mixed at ratios predetermined by ternary phase diagrams. The excipients were weighed in screw-capped borosilicate vials and the mixture was heated up to 55 °C, which is 5 °C above the melting point of the solid excipients, and constantly stirred at 700 rpm to give a homogenous mixture. All the formulations were kept for 24 h at ambient temperature to reach equilibrium before characterization studies. The formulations containing the peptide or Dox HCl were prepared by mixing the peptide, Dox HCl or both after the formulations have reached equilibrium, followed by dilution with PBS or cell culture media.

SMEDDS formulations were evaluated in terms of organoleptic properties for physical stability (i.e. phase separation, creaming, coalescence etc.). Liquid crystal formation was assessed under Polarized Light Microscope (Leica DM EP, Germany). The droplet size and zeta potential of the formulations were determined using Malvern Nanosizer ZS 2000 (United Kingdom).

2.3. Cell culture and colorimetric viability assay

MDA-MB-231 cell line (ATCC, LGC Promochem, Rockville, MD, USA) was cultured in high-glucose DMEM whereas 4T1 cell line was grown in RPMI 1640 media. The media was supplemented with L-glutamine (4 mM), 1% penicillin and streptomycin (Biochrom, Berlin, Germany) and 10% fetal bovine serum (Biological Industries, Kibbutz Beit HaEmek, Israel) and maintained in a humidified incubator with 5% CO_2 at 37 °C.

In vitro anti-cancer efficacy of LyP-1 and/or Dox HCl either in solution or in the formulations was tested on MDA-MB-231 and 4T1 breast cancer cells. The cells were seeded into (MDA-MB-231 and 4T1, 2×10^4 cells/well) 96-well plates. The next day serial dilutions of the agents and the formulations were applied and incubated for 24 and 48 h. The amount of viable cells was assessed with 3-(4,5-dimethylthiazol-2-yl)-2,5-diphenyltetrazolium bromide (MTT) assay. Briefly, MTT solution was added into the wells at a concentration of 1 μg/mL, and after 4 h of incubation, lysis solution (23% sodium dodecyl sulfate in N,N-Dimethylformamide) was added to dissolve the formazan crystals. The absorbance was measured at 570 nm using a plate reader (VersaMax™ Microplate Reader, Molecular Devices, USA).

2.4. Cellular uptake studies

The uptake of LyP-1 was evaluated on 4T1 cells, which has been reported to express the p32 receptor [54,55]. 4T1 cells (2×10^5 cells/mL) were incubated with the LyP-1 labelled with a fluorescent probe (LyP-1-FAM) at 1 μM, 3 μM, 9 μM, and 27 μM concentrations, which were either prepared in culture medium or in SMEDDS formulations. FAM alone was used as a control. Upon 1 and 5 h incubation at 4 °C and 37 °C, the cells were washed and suspended in phosphate buffered saline (PBS) and the median fluorescence intensity (MFI) values were measured utilizing a flow cytometer (BD FACSAria II, USA).

2.5. Reverse transcription-polymerase chain reaction (RT-PCR)

RT-PCR was performed to confirm the expression of p32 in 4T1 cells and in the tumor tissues established in mice. Isolated RNA (RNeasy Mini Kit, QIAGEN, Germany) was converted to cDNA by reverse transcription using oligo (dT) primers (QuantiTect Reverse Transcription Kit, QIAGEN, Germany). The primer oligonucleotide sequences used were as follows: mouse p32 forward 5′- CGGTCGTCCTTCCCTCTG-3′, reverse 5′-AACGAAGGCCTTGTCTCCTTC-3′; mouse β-actin forward 5′-CACTG TCGAGTCGCGTCCA-3′, and reverse 5′-CCATCACACCCTGGTGCCTA-3′. The products (mouse p32, 278 bp; mouse b-actin, 214 bp) were run on agarose gel (2%) electrophoresis, stained with ethidium bromide and documented under UV light.

2.6. Western-Blot analysis

The protein levels of p32 in the MDA-MB-231 and 4T1 cell lines and in the 4T1 tumors established during in vivo studies were assessed by Western-Blot. The cells (2×10^6) were washed with ice-cold PBS, lysis buffer (RIPA, 400 μL) was added and then the cells were harvested by scraping. All procedures were performed on ice. Tumor tissues were homogenized in the lysis buffer (200 μL per 5 mg tissue) with zircon beads (BeadBeater, Biospec, USA). The lysates were centrifuged for 15 min at 12.500 rpm at 4 °C and supernatant fractions were collected. The bicinchoninic acid (BCA) assay was used for determining the amount of protein. The samples were denatured (5 min at 95 °C), and equal amount of protein was loaded on polyacrylamide gel electrophoresis (SDS-PAGE) after dilution with 2× Laemmli sample buffer.

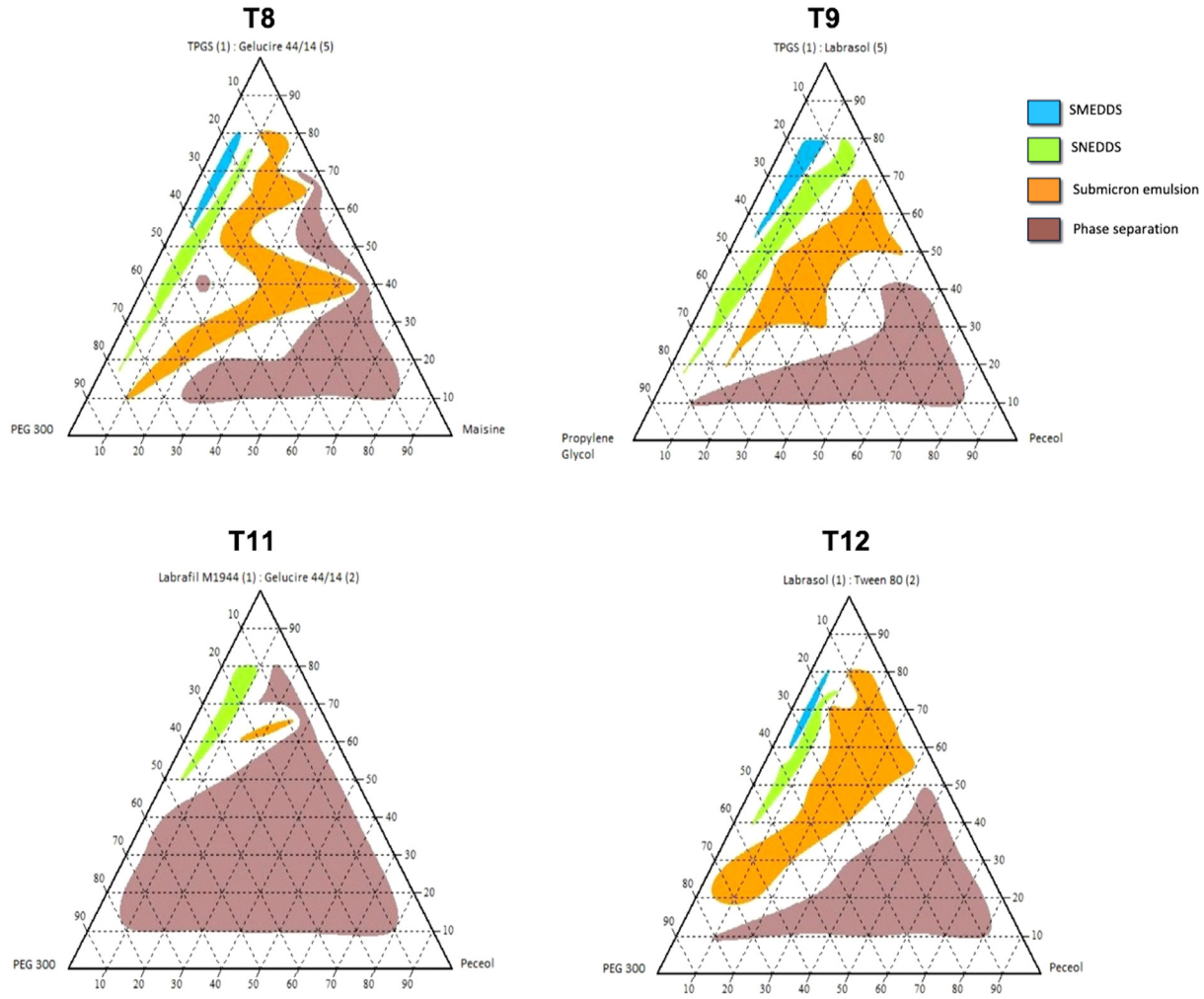

Fig. 1. Ternary phase diagrams of selected SMEDDS formulations A. T8 B. T9 C. T11 D. T12. The formulations are coded as the number of ternary phase diagram (T) - the formulation number in the same diagram (F).

The separated proteins on the gel were transferred to polyvinylidene fluoride membrane (PVDF, 0.45 µm) by semi-dry transfer (Pierce Fast Semi-Dry Blotter, Thermo Scientific, Germany). Anti-p32 (60.11; Abcam, USA) (1:200 dilution) and goat anti-mouse IgG (GAM- HRP; BioLegend, USA) (1:5000 dilution) were used as the primary and secondary antibodies, respectively. Imaging was performed with SuperSignal West Femto Maximum Sensitivity Substrate (Thermo Scientific, Germany) and images were taken using a Kodak Gel Logic 1500 Imaging System (Carestream Health, Rochester, NY, USA).

2.7. In vivo experiments with 4T1 Tumor-bearing mice

Eight-week-old inbred female BALB/c mice (Kobay Inc., Ankara, Turkey) were housed under environmentally controlled standard conditions. All procedures were approved by the Institutional Ethical Committee of Hacettepe University, Ankara, Turkey (Approval Number: 2012/14-11). 4T1 breast cancer cells (2.5×10^4) were inoculated into mammary fat pads of the mice. When the mean diameter of the tumors reached to ~0.4 cm, the mice were separated into 6 experimental groups. Three groups received LyP-1 in PBS (3 mg/kg, n = 7), Dox HCl in PBS (5 mg/kg, n = 8), and the combination of LyP-1 and Dox HCl in PBS (3 mg/kg LyP-1 and 5 mg/kg, Dox HCl, n = 8). Another three groups were treated with LyP-1 in SMEDDS (3 mg/kg, n = 8), Dox HCl in SMEDDS (5 mg/kg, n = 8), and the combination of LyP-1 and Dox HCl in SMEDDS (3 mg/kg LyP-1 and 5 mg/kg, Dox HCl, n = 8). The composition of the formulation (T9-F21) used in animal studies is as follows: TPGS: Labrasol (1:5) (55%), Peceol (5%), propylene glycol (40%). These formulations were administered twice a week by intraperitoneal route. Geometric mean of the tumor diameters was measured for 4 weeks.

2.8. Histopathological evaluation

Histopathological changes and metastatic foci were evaluated in the tumors, mesenteric lymph nodes, lungs, and liver samples which were resected and fixed in 10% formalin solution. All tissue samples were embedded in paraffin and, 4 µm sections were cut and stained with routine hematoxylin and eosin (H&E) protocol. Complete sampling of liver and lungs was performed for all groups. The evaluation was performed using a conventional light microscopy (Olympus CX41, USA) by a specialist in pathology.

2.9. Analysis of biodistribution

The 4T1 tumor-bearing or healthy (control) mice were intraperitoneally injected with LyP-1-FAM solution (200 µL) in PBS (3 mM) or the LyP-1-FAM in the SMEDDS formulation (3 mM). After 16 h, the animals were sacrificed and peripheral blood, peritoneal fluid, liver, mammary and mesenteric lymph nodes, and tumor tissue samples were collected. The cells were freshly isolated by mechanical agitation of the tissues, filtered through 0.45 µm pore-sized filters and subjected to gradient separation according to Histopaque®1119 protocol. These

isolated cells were analyzed by flow cytometry (488 nm excitation) and fluorescence intensities from LyP-1-FAM-labelled cells were obtained. Alternatively, the tissues were finely sliced (~3 mm) and fluorescence emission was visualized under UV light (Kodak Gel Logic 1500 Imaging System, Carestream).

2.10. Statistical analysis

Statistical analysis of non-parametric groups was performed utilizing the Kruskall-Wallis test among two groups and the Mann-Whitney U test when there were more than two groups. The groups, which exhibited statistical difference, were further evaluated by multiple comparison tests. The results of the in vivo studies were evaluated by Generalized Estimating Equations (GEE) to determine the differences among the repeated measurements within the groups. The statistical difference between qualitative data was determined with Chi Square test. All results were expressed as mean ± SD, unless indicated otherwise.

3. Results

3.1. Preparation and characterization of the SMEDDS formulations

The combinations of excipients giving stable SMEDDS formulations were determined using ternary phase diagrams (Fig. 1). The stable microemulsion regions for all mixtures studied were found to be consisting of 50 – 80% surfactant, 10 – 45% co-solvent and 5 – 15% oil. The most stable formulations were formed when Peceol or Maisine were used as the oil phase, PEG 300 or Propylene Glycol as the co-solvent, TPGS:Gelucire 44/14, TPGS:Labrasol, Labrasol:Tween 80 or Labrafil M1944:Gelucire 44/14 as the surfactant mixtures. The selected formulations contained either Maisine (5%), PEG 300 (40%) and TPGS:Gelucire 44/14 (1:5 ratio, 55%); Peceol (5%), propylene glycol (35%), and TPGS:Labrasol (1:5 ratio, 60%); Peceol (5%), propylene glycol (40%), and TPGS:Labrasol (1:5 ratio, 55%); Peceol (5%), propylene glycol (45%), and TPGS:Labrasol (1:5 ratio, 50%) or Peceol (5%), PEG 300 (35%), and Labrasol:Tween 80 (1:2 ratio, 60%).

The selected formulations formed clear, stable microemulsions with no sign of physical instability such as phase separation, creaming, coalescence or turbidity (data not shown). In addition, no crystal liquid formation was observed, which could occur due to high surfactant content of the SMEDDS formulations. The droplet size of the SMEDDS formulations was found to be in the range of 15.36 – 19.16 nm. Addition of the peptide in the formulations had no effect on droplet size except for formulations T8-F21, T9-F21 and T12-F17 ($p > 0.05$), and the droplet size of the peptide-containing formulations was in the range of 14.95–76.43 nm.

3.2. In vitro cytotoxic efficacy of LyP-1 and Dox HCl administered in the SMEDDS formulations on p32-expressing breast cancer cells

In order to confirm the presence of p32, the specific receptor for LyP-1, on MDA-MB-231 and 4T1 cells, both gene and protein expression were analyzed. Both 4T1 and MDA-MB-231 cells expressed the p32 protein (32 kDa), and it was higher in MDA-MB-231 cells than in 4T1 cells. In the tumor tissue samples obtained from the mice which were previously inoculated with 4T1 cells, p32 was also detectable (Fig. 2A). The presence of p32 in the 4T1 cells and tumors was also evaluated in terms of gene expression. The p32 transcripts were highly amplified both in the 4T1 cells and tumors (Fig. 2B).

Following the confirmation of the cell lines to be positive for p32, the cytotoxic effect of Dox HCl and LyP-1 combination was evaluated for 48 h on 4T1 and MDA-MB-231 cell lines. The concentration of Dox HCl was held constant at 0.15 μM in order to evaluate the additive effect of LyP-1, which was used at increasing concentrations. A dose-dependent synergistic effect was observed with LyP-1 as it increased the

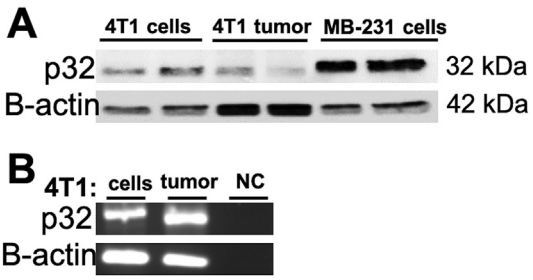

Fig. 2. The expression of p32 in the MDA-MB-231 and 4T1 breast cancer cell lines, and the 4T1 tumor tissues studied. (A) p32 protein (32 kDa) levels were studied by Western-Blot. B-actin (42 kDa) was used as house-keeping protein as loading control. Each sample was studied in duplicates. (B) p32 expression in the 4T1 cells and tumors was evaluated by RT-PCR. The p32 amplicons were visualized after agarose gel electrophoresis. B-actin was amplified as house-keeping gene. NC: negative control.

anti-tumor cell activity of Dox HCl on MDA-MB-231 cell line starting from 31.25 μM concentration in 48 h (Fig. 3A). For the 4T1 cell line, this effect was detected with 125 μM and 250 μM LyP-1 when combined with 0.15 μM Dox HCl (Fig. 3B). LyP-1 influenced the MDA-MB-231 more potently than the 4T1 cell line, which could be attributed to higher expression levels of p32 in the MDA-MB-231 as compared to 4T1 (Fig. 2A). Even though administration of Dox HCl and LyP-1 treatment with the SMEDDS formulations decreased the amount of viable breast cancer cells, the effect of LyP-1 was not clear potentially due to masking by the high potency of Dox HCl when administered in the SMEDDS (Fig. 4).

3.3. The efficacy of cellular uptake of LyP-1 in the SMEDDS formulation

The uptake of LyP-1-FAM prepared in solution and in the SMEDDS formulation by the 4T1 cells was concentration- and time-dependent at 37 °C (Fig. 5A). After 1 h of incubation with 27 μM LyP-1-FAM in solution, the median fluorescence intensity (MFI) was 101 ± 7.7, while the intensity increased to 138.12 ± 3.28 in 5 h ($p < 0.01$). The uptake was higher when the peptide was applied in the SMEDDS formulations (MFI, 116.75 ± 0.75 in 1 h; 153.25 ± 9.01 in 5 h), (Fig. 5B and C).

Since the energy-dependent endocytic cellular uptake pathways are hampered at 4 °C [56], additional studies were performed at this temperature to support the observations on the specificity of LyP-1 as a ligand mediating cellular entry. Therefore, the fluorescence intensity obtained at 37 °C indicates both the internalized and cell surface-bound LyP-1 peptide whereas at 4 °C the majority of fluorescence signals would only derive from the peptide that was bound onto the cell membrane (Fig. 5B and C). Accordingly, the fluorescence intensity of the peptide in solution was 5.6 ± 2.5 after 1 h incubation at 4 °C and increased to 57.5 ± 9.1 at 37 °C, (a 124.6% increase, $p < 0.01$). A similar trend was also observed when the peptide was prepared in the SMEDDS formulation; the fluorescence intensity increased from 25.3 ± 3.1 to 59.5 ± 20.6 at 4 °C and 37 °C, respectively, (a 135.17% increase, $p < 0.01$). Following 5 h of incubation, similar results were obtained which corresponded to the temperature-dependent uptake at 1 h. Accordingly, for the LyP-1-FAM in solution, approximately 24% increase was obtained when the results at 4 °C and 37 °C were compared ($p < 0.01$). Notably, for the LyP-1-FAM in the SMEDDS, this increase was even more significant (~95.1%, $p < 0.0001$) (Fig. 5B and C). Therefore, the uptake of the peptide was enhanced when administered in the SMEDDS formulations especially following extended incubation at 37 °C. In addition, the reduction in the fluorescence intensity values at 4 °C could be attributed to the receptor-mediated endocytosis of the peptide potentially through the p32 pathway.

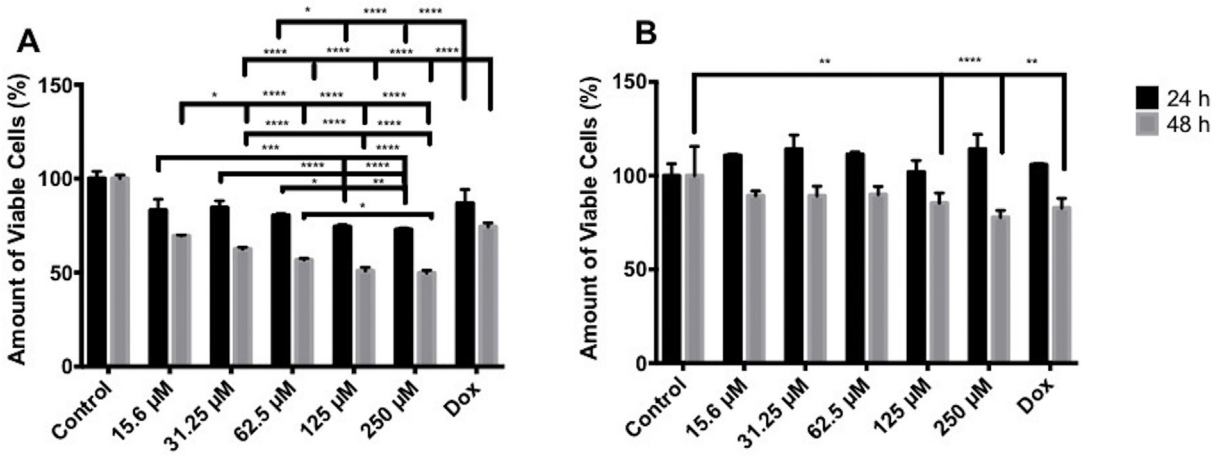

Fig. 3. The amount of viable cells after treatment with Dox HCl and LyP-1 combination in solution on (A) MDA-MB-231, (B) 4T1 cell line (*$p < 0.05$** $p < 0.01$; *** $p < 0.001$; **** $p < 0.0001$, n = 4). All peptide concentrations were administered with 0.15 μM of Dox HCl. Dox stands for 0.15 μM Dox HCl solution. Change in the amount of viable cells (%) were expressed as percentage of control cells ± SD.

3.4. Combination of LyP-1 and Dox HCl in the SMEDDS formulations decelerates tumor growth and metastasis

The mice bearing 4T1 breast tumors were administered with LyP-1 and/or Dox HCl in PBS solution or in the SMEDDS formulations and were followed for 14 days. The PBS-treated control group had a survival rate of 66% by the day 28. On the other hand, the animals administered with the blank SMEDDS formulations had the lowest survival rate (57.14%). The groups treated with LyP-1 in solution and LyP-1 in the SMEDDS formulations showed 85.7% and 87.5% survival rates, respectively. All the other tumor-bearing animal groups survived through the study period.

The combination of Dox HCl and LyP-1 either in solution or in the SMEDDS formulations significantly reduced the tumor growth when compared to the tumor-bearing animals treated with Dox HCl in solution or in the SMEDDS formulations (Fig. 6). In addition, even though not reaching to the level of statistical significance, the tumors tended to have smaller diameters when treated with LyP-1 (Fig. 6). Thus, combination of LyP-1 with Dox HCl appeared to negatively influence tumor progression. Expectedly, the tumor burden in the groups treated with the Dox HCl in SMEDDS, the Dox HCl and LyP-1 in solution, and Dox HCl and LyP-1 in the SMEDDS formulations was less than the untreated control animals (data not shown). Therefore, the anti-tumor activity of Dox HCl and LyP-1 in the SMEDDS formulations and in solution was demonstrated.

The breast cancer metastases were evaluated in the liver, lungs and lymph nodes of the tumor-bearing animals. The animals that received the combination of Dox HCl and LyP-1 in the SMEDDS formulations displayed the lowest frequency of metastasis (12.5%), in contrast to LyP-1 in the SMEDDS formulations ($p < 0.05$), Dox HCl in solution and Dox HCl in SMEDDS ($p < 0.2$) (Table 1). The number of metastatic foci was similarly reduced whether Dox HCl was administered in solution (25%) or in the SMEDDS formulation (25%) (Table 1). Collectively, the SMEDDS formulations developed in this study endorsed the anti-cancer efficacy of Dox HCl and LyP-1 both in terms of tumor growth and metastatic spread.

3.5. LyP-1 in the SMEDDS formulations preferentially accumulates in the tumor tissue

The tumor-bearing or healthy mice were injected with LyP-1-FAM and tissue samples of liver, mammary lymph nodes, mesenteric lymph nodes, and tumors were collected. The fluorescence intensity obtained from the tissues showed that the peptide in the SMEDDS formulations preferentially accumulated in the tumor tissues (Fig. 7A). Alternatively, LyP-1 in solution was distributed in the liver, peripheral blood, peritoneal fluid, tumor and mesenteric lymph nodes. A high amount of the peptide was found in the mesenteric lymph node, liver, peripheral blood and tumor when administered in the SMEDDS formulations (Fig. 7A). Additionally, the florescence intensity of the LyP-1-FAM in solution was compared to that in the SMEDDS formulations by a flow cytometry approach at the cellular level. The LyP-1-FAM in the

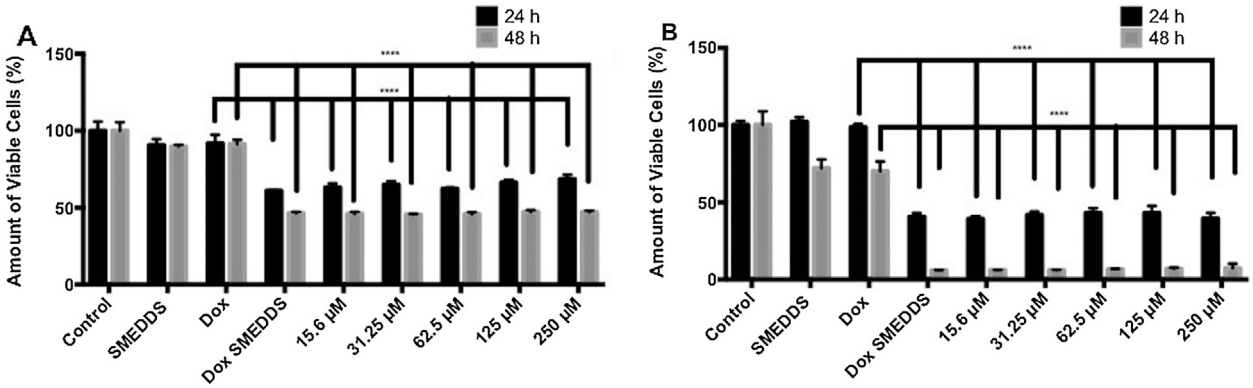

Fig. 4. The amount of viable cells after treatment with Dox HCl and LyP-1 combination in SMEDDS on (A) MDA-MB-231, (B) 4T1 cell line (**** $p < 0.0001$, n = 4). All peptide concentrations were administered with 0.15 μM of Dox HCl. Dox stands for 0.15 μM Dox HCl solution. Change in the amount of viable cells (%) were expressed as percentage of control cells ± SD.

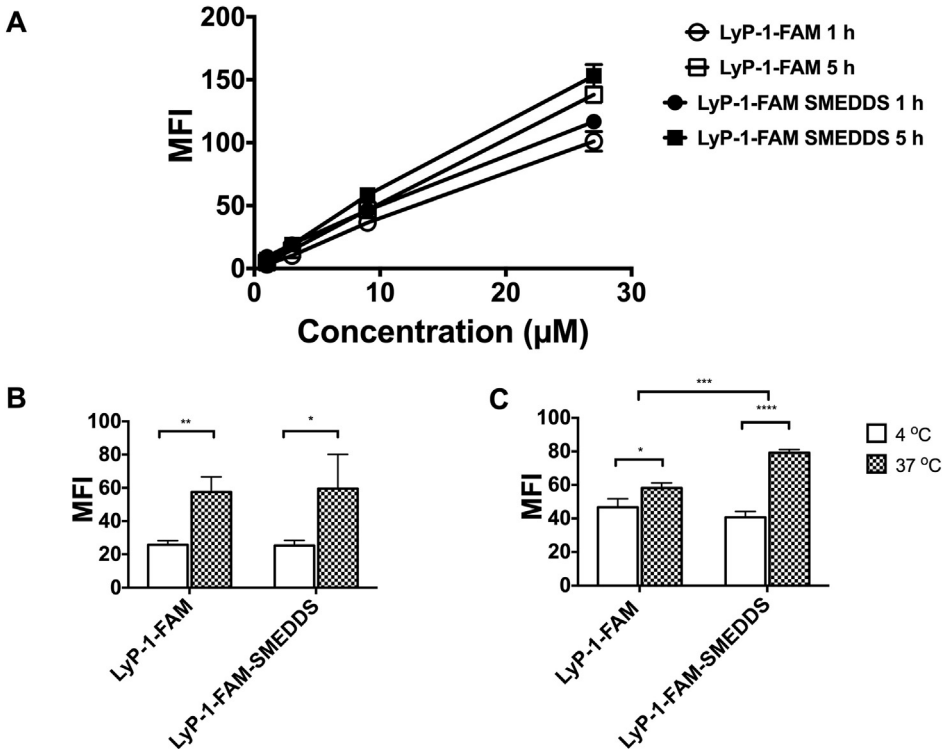

Fig. 5. The uptake of LyP-1-FAM by the 4T1 cells was analyzed by flow cytometry. (A) The influence of time and concentration of LyP-1-FAM was evaluated. The uptake of LyP-1-FAM in solution and SMEDDS formulations was evaluated (B) after 1 h-long and (C) 5 h-long incubations at 37 °C and 4 °C, (n = 3). Data are presented as mean fluorescent intensity ± SD.

SMEDDS formulations in the cell suspensions obtained from mesenteric lymph nodes and from the tumors possessed high-level fluorescence which confirmed the tissue biodistribution data (Fig. 7B and C).

The in vivo administrations were performed via the intraperitoneal route and numerous macrophages, which are known as the major cell type to collect and interfere with the dissemination of exogenous materials, were present in the peritoneal cavity [57]. Peritoneal lavages were performed, and the presence of LyP-1-FAM fluorescence was examined in CD206-positive macrophages. When the peptide was administered in solution, its accumulation in the macrophages was higher than when the peptide was in the SMEDDS formulations. LyP-1-FAM was distributed throughout the total immune cells in the peritoneal cavity but not much in the macrophages (Supplementary Fig. 1). The mesenteric lymph node uptake of the peptide was found to be highest when delivered in the SMEDDS formulations (Fig. 7B). The uptake in the liver was evaluated by means of immune cell type; the total liver cells were found to show higher fluorescence intensity in both healthy and tumor-bearing mice. In the peripheral blood, the highest intensity was recorded in the tumor-bearing mice that were administered with LyP-1-FAM in the SMEDDS formulations (Supplementary Fig. 2). The distribution in total splenocytes and macrophages in the spleen were found to be similar; however, the escape potential from the macrophages was observed when the peptide was administered in the

Table 1
% of mice with metastasis after histopathological evaluation.

	Solution	SMEDDS
LyP-1	50% (3/6)[+]	71.4% (5/7)[*]
Dox HCl	25% (2/8)[**]	25% (2/8)[**]
LyP-1 + Dox HCl	37.5% (3/8)	12.5% (1/8)

* $p < 0.05$ and,
** $p < 0.2$ *vs* LyP-1 + Dox HCl SMEDDS.
[+] (number of animals with metastasis/total number of animals in group).

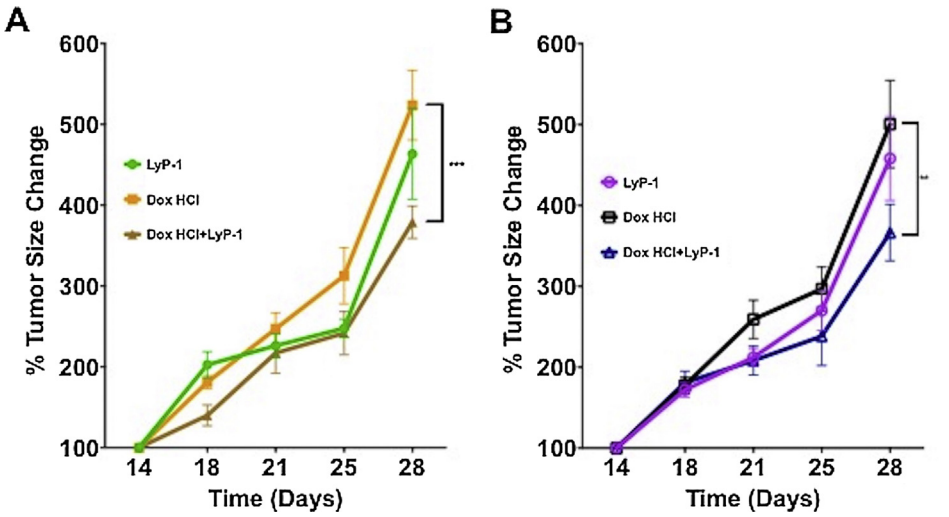

Fig. 6. The % change in tumor sizes of the treatment groups of tumor-bearing BALB/c mice (**$p < 0.01$; *** $p < 0.001$). Data are presented as mean ± SD. The treatment groups were administered twice a week with A. LyP-1 in PBS (3 mg/kg, n = 7), Dox HCl in PBS (5 mg/kg, n = 8) or the combination of these chemotherapeutics (3 mg/kg LyP-1 + 5 mg/kg Dox HCl, n = 8) in PBS, and B. LyP-1 in SMEDDS (3 mg/kg, n = 8), Dox HCl in SMEDDS (5 mg/kg, n = 8) or the combination of these chemotherapeutics (3 mg/kg LyP-1 + 5 mg/kg Dox HCl, n = 8) in SMEDDS formulation. C. % of mice with metastasis after histopathological evaluation.

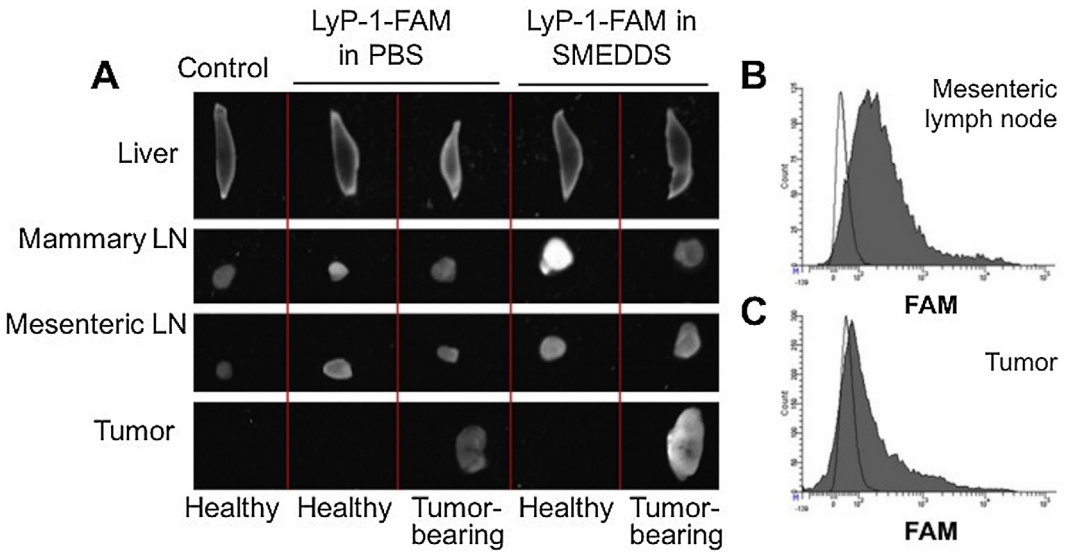

Fig. 7. A. UV images of the tissues from healthy and tumor bearing mice (liver, mammary lymph node, mesenteric lymph node, tumor) treated with either LyP-1-FAM solution or LyP-1-FAM SMEDDS. B. Flow cytometry histogram plots showing fluorescence intensity of LyP-1-FAM solution (plot in white) and LyP-1-FAM SMEDDS (plot in gray) in mesenteric lymph node. C. Flow cytometry histogram plots showing fluorescence intensity of LyP-1-FAM solution (plot in white) and LyP-1-FAM SMEDDS (plot in gray) in tumor tissue.

SMEDDS formulations to the tumor-bearing mice (data not shown).

4. Discussion

4.1. Preparation and characterization of the SMEDDS formulations

One of the most critical steps for the formation of self-micro-emulsifying drug delivery systems is the selection of excipients to form the desired microemulsions in accordance with the pharmaceutical purpose of the formulation [37]. Even the excipients, which are especially produced for self- emulsification, may not end up with a suitable SMEDDS formulation. Therefore, preformulation studies are crucial for achieving the optimum formulation. The self-emulsification could be affected from the oil/surfactant properties, surfactant ratio, and oil/surfactant percentage [34,40]. All the excipients selected for this study were suitable for both parenteral and oral administration. The excipient mixtures, which formed droplets under 100 nm were selected for further studies to increase the lymphatic absorption of the peptide.

The zeta potential values of the blank formulations were approximately neutral due to the high proportion of the non-ionic surfactants. LyP-1 is a nonapeptide (CGNKRTRGC) with positive charged amino acids, such as lysine and arginine; thus, making the net charge of the peptide slightly positive. The zeta potential of the peptide formulations was approximately neutral as expected with no significant effect of the charge of the peptide. Stable SMEDDS with droplet size between 12.92 ± 0.07 and 294.07 ± 1.77 nm were obtained. The SMEDDS formulations for further studies were selected by considering the droplet size distribution, physical stability and surfactant concentration. The T9-F21 formulation, which was used for animal studies had a droplet size of 15.36 ± 0.08 nm and 25.01 ± 1.93 nm in the absence and presence of the peptide, respectively [58–60].

4.2. In vitro cytotoxic efficacy of LyP-1 and Dox HCl administered in the SMEDDS formulations on p32-expressing breast cancer cells

MDA-MB-231 cell line was treated with the blank SMEDDS formulations in order to confirm that the anticancer activity observed was solely due to the peptide but not the formulation. After 24 and 48 h of incubation, the blank formulations and the control group led to similar cell viability, indicating that the bioactivity was in fact due to LyP-1.

The anticancer activity of the peptide was evaluated in the range of 15.6 – 250 μM, and dose-dependent activity could be clearly seen on the MDA-MB-231 cell line. This data was supported by the Western-Blot analyses confirming the higher expression of p32 receptor in this cell line. Up until now, the in vitro anticancer activity of the peptide was only shown using the MDA-MB-435 cell line [10], and with the present work, it was also shown utilizing the MDA-MB-231 and 4T1 cell lines and supported with the in vivo data.

The effect of combination therapy was assessed using the lowest effective concentration of Dox HCl (0.15 μM) to evaluate the possible synergistic effect of the peptide in both the 4T1 and MDA-MB-231 cell lines. The addition of LyP-1 (250 μM) in the treatment regimen increased the efficacy of Dox HCl, leading to a decrease in cell viability from 74.3% to 49.6% following 48 h of incubation in the MDA-MB-231 cell line.

The effect of the SMEDDS formulation in the combination therapy was observed by delivering LyP-1 and Dox HCl in the SMEDDS formulations. Although the concentration-dependent anticancer effect of the peptide appeared to be interfered by the formulation, the efficacy of Dox HCl appeared to increase when delivered in the SMEDDS formulation.

4.3. The efficacy of cellular uptake of LyP-1 in the SMEDDS formulations

LyP-1-FAM was efficiently uptaken by the 4T1 cells. It appeared that the peptide uptake by the 4T1 cells was higher when delivered in the SMEDDS as compared to the one in solution. The temperature-dependent uptake of the LyP-1-FAM confirmed the internalization of the peptide via energy-dependent pathways (i.e. receptor-mediated endocytosis). The administration of the peptide in the SMEDDS formulations enabled both easy transport through enhanced cellular permeation and sustained peptide stability.

4.4. p32 expression

Western-Blot analyses and polymerase chain reaction confirmed the expression of p32 expression in the cell lines and tumor tissue samples. The expression of p32 was observed to be higher in the MDA-MB-231 cell line when compared to the 4T1 cell line. These results are in parallel with the in vitro cell viability data, which implied the prominent

concentration-dependent toxicity of LyP-1 in the MDA-MB-231 cell line as a result of p32 expression.

4.5. Combination of LyP-1 and Dox HCl in the SMEDDS formulations decelerates tumor growth and metastasis

The tumor model used for in vivo studies is a commonly preferred model, which is superior for its high tumor progression rate and formation of metastasis. This model is called a ″triple negative model″ representing 15% of the breast cancer cases in humans that do not express the PR, ER and HER2 receptors [61]. The progression is aggressive, and the potential of metastasis is high as it leads to metastasis in the liver, lung, lymph nodes etc. when administered via the mammary fat pad [62]. This aggressive tendency was also observed in the 28^{th} day of inoculation with loss of animals bearing large tumors in the study groups. Despite the aggressive progression of the tumors, the difference in % change in tumor size among the control groups (PBS and blank SMEDDS) and the combination therapy groups were found to be significant. The difference between the Dox HCl and the combination therapy (Dox HCl + LyP-1), both in solution and in the SMEDDS formulation, demonstrated the synergistic effect of the peptide. This phenomenon could be explained by the ″bystander effect″in addition to the anticancer activity of the peptide. LyP-1 and RGD peptides have been shown to exert an additional effect for the drug, which they are administered together even when there is no covalent bond between the drug and the peptide [63]. In the present work, the same effect was observed in the combination therapy when LyP-1 was delivered together with Dox HCl.

4.6. LyP-1 in the SMEDDS preferentially accumulates in the tumor tissue

Intraperitoneal administration is an alternative for i.v. injection in small laboratory animals, and it has similar pharmacokinetic aspects with respect to oral administration. The absorption of the drug is slower as compared to the one obtained with i.v. injection, and drug molecules absorbed by the mesenteric vessels reach the liver via the portal vein [64]. The absorption of the peptide delivered in the SMEDDS formulations followed the regular absorption pathway in the tumor-bearing mice. The high level of accumulation in the mesenteric lymph nodes supported the lymphatic targeting achieved by LyP-1. The accumulation of the peptide in the liver when delivered in both the solution and the SMEDDS formulations was an expected result due to i.p. administration. The CD206 labeling showed that the peptide accumulated less in the macrophages when compared to the total immune cells in the samples collected from the peritoneal cavity and liver following administration of the SMEDDS formulations in tumor-bearing mice. This result demonstrated the possibility of the escape of the peptide in the SMEDDS formulations from the macrophages in the areas especially containing high population of immune cells.

The highest amount of LyP-1 in the systemic circulation was found when the peptide was delivered in the SMEDDS formulation in tumor-bearing mice implying the possible absorption enhancing of the formulation excipients. Similarly, the accumulation of the peptide in the tumor tissues also increased when the peptide was administered in the SMEDDS formulation. The high levels of peptide accumulation in the tumor tissue macrophages could be explained by the expression of the p32 receptor on the tumor-related macrophages leading to LyP-1 accumulation in the tumor macrophages, tumor lymphatics and tumor cells following i.v. injection [9,10,65]. The UV images also confirmed the accumulation of LyP-1 in the SMEDDS formulation in the mesenchymal lymph nodes and tumor tissue in the tumor-bearing mice.

5. Conclusions

Stable lipid-based drug delivery systems (SMEDDS) with droplet size under 100 nm have been developed, and the potential of these novel drug delivery systems to combat tumor growth in breast cancer has been shown in tumor bearing mice. LyP-1 and Dox HCl have been successfully co-administrated in the same delivery system without any further chemical process. This approach could be applicable for the delivery of other anticancer drugs.

Acknowledgement

This project was supported by TUBITAK (The Scientific and Technological Research Council of Turkey; grant number: SBAG 1002-113S569) and Hacettepe University, Turkey, Scientific Research Projects Funding Program (grant number: THD-2017-11642).

Appendix A. Supplementary material

Supplementary data to this article can be found online at https://doi.org/10.1016/j.ejpb.2019.01.017.

References

[1] E. Perez-Herrero, A. Fernandez-Medarde, Advanced targeted therapies in cancer: drug nanocarriers, the future of chemotherapy, Eur. J. Pharm. Biopharm. 93 (2015) 52–79.
[2] T. Lammers, F. Kiessling, W.E. Hennink, G. Storm, Drug targeting to tumors: principles, pitfalls and (pre-) clinical progress, J. Control. Release 161 (2012) 175–187.
[3] G.V. Rosland, A.S. Engelsen, Novel points of attack for targeted cancer therapy, Basic Clin. Pharmacol. Toxicol. 116 (2015) 9–18.
[4] P. Saharinen, T. Tammela, M.J. Karkkainen, K. Alitalo, Lymphatic vasculature: development, molecular regulation and role in tumor metastasis and inflammation, Trends Immunol. 25 (2004) 387–395.
[5] N.L. Trevaskis, L.M. Kaminskas, C.J. Porter, From sewer to saviour - targeting the lymphatic system to promote drug exposure and activity, Nat. Rev. Drug Discovery 14 (2015) 781–803.
[6] S.P. Wahal, M.M. Goel, R. Mehrotra, Lymphatic vessel assessment by podoplanin (D2–40) immunohistochemistry in breast cancer, J. Cancer Res. Ther. 11 (2015) 798–804.
[7] D.R. Christianson, A.S. Dobroff, B. Proneth, A.J. Zurita, A. Salameh, E. Dondossola, J. Makino, C.G. Bologa, T.L. Smith, V.J. Yao, T.L. Calderone, D.J. O'Connell, T.I. Oprea, K. Kataoka, D.J. Cahill, J.E. Gershenwald, R.L. Sidman, W. Arap, R. Pasqualini, Ligand-directed targeting of lymphatic vessels uncovers mechanistic insights in melanoma metastasis, Proc. Nat. Acad. Sci. United States Am. 112 (2015) 2521–2526.
[8] L.C. Dieterich, M. Detmar, Tumor lymphangiogenesis and new drug development, Adv. Drug Deliv. Rev. 99 (2016) 148–160.
[9] P. Laakkonen, K. Porkka, J.A. Hoffman, E. Ruoslahti, A tumor-homing peptide with a targeting specificity related to lymphatic vessels, Nat. Med. 8 (2002) 751–755.
[10] P. Laakkonen, M.E. Akerman, H. Biliran, M. Yang, F. Ferrer, T. Karpanen, R.M. Hoffman, E. Ruoslahti, Antitumor activity of a homing peptide that targets tumor lymphatics and tumor cells, Proc. Nat. Acad. Sci. United States Am. 101 (2004) 9381–9386.
[11] J. Hamzah, V.R. Kotamraju, J.W. Seo, L. Agemy, V. Fogal, L.M. Mahakian, D. Peters, L. Roth, M.K. Gagnon, K.W. Ferrara, E. Ruoslahti, Specific penetration and accumulation of a homing peptide within atherosclerotic plaques of apolipoprotein E-deficient mice, Proc. Nat. Acad. Sci. United States Am. 108 (2011) 7154–7159.
[12] E. Ruoslahti, Peptides as targeting elements and tissue penetration devices for nanoparticles, Adv. Mater. 24 (2012) 3747–3756.
[13] E. Ruoslahti, Tumor penetrating peptides for improved drug delivery, Adv. Drug Deliv. Rev. (2016).
[14] Z. Yan, C. Zhan, Z. Wen, L. Feng, F. Wang, Y. Liu, X. Yang, Q. Dong, M. Liu, W. Lu, LyP-1-conjugated doxorubicin-loaded liposomes suppress lymphatic metastasis by inhibiting lymph node metastases and destroying tumor lymphatics, Nanotechnology 22 (2011) 415103.
[15] Z. Yan, F. Wang, Z. Wen, C. Zhan, L. Feng, Y. Liu, X. Wei, C. Xie, W. Lu, LyP-1-conjugated PEGylated liposomes: a carrier system for targeted therapy of lymphatic metastatic tumor, J. control. Release: Off. J. Control. Release Soc. 157 (2012) 118–125.
[16] T.P. Herringson, J.G. Altin, Effective tumor targeting and enhanced anti-tumor effect of liposomes engrafted with peptides specific for tumor lymphatics and vasculature, Int. J. Pharm. 411 (2011) 206–214.
[17] J.H. Park, G. von Maltzahn, M.J. Xu, V. Fogal, V.R. Kotamraju, E. Ruoslahti, S.N. Bhatia, M.J. Sailor, Cooperative nanomaterial system to sensitize, target, and treat tumors, Proc. Nat. Acad. Sci. United States Am. 107 (2010) 981–986.
[18] J.W. Seo, H. Baek, L.M. Mahakian, J. Kusunose, J. Hamzah, E. Ruoslahti, K.W. Ferrara, (64)Cu-labeled LyP-1-dendrimer for PET-CT imaging of atherosclerotic plaque, Bioconjugate Chem. 25 (2014) 231–239.
[19] E.H. Lempens, M. Merkx, M. Tirrell, E.W. Meijer, Dendrimer display of tumor-homing peptides, Bioconjugate Chem. 22 (2011) 397–405.
[20] F. Yan, X. Li, C. Jiang, Q. Jin, Z. Zhang, R. Shandas, J. Wu, X. Liu, H. Zheng, A novel microfluidic chip for assessing dynamic adhesion behavior of cell-targeting

microbubbles, Ultrasound Med. Biol. 40 (2014) 148–157.
[21] F. Yan, X. Li, Q. Jin, C. Jiang, Z. Zhang, T. Ling, B. Qiu, H. Zheng, Therapeutic ultrasonic microbubbles carrying paclitaxel and LyP-1 peptide: preparation, characterization and application to ultrasound-assisted chemotherapy in breast cancer cells, Ultrasound Med. Biol. 37 (2011) 768–779.
[22] X. Li, Q. Jin, T. Chen, B. Zhang, R. Zheng, Z. Wang, H. Zheng, LyP-1 ultrasonic microbubbles targeting to cancer cell as tumor bio-acoustics markers or drug carriers: targeting efficiency evaluation in, microfluidic channels, IEEE Engineering in Medicine and Biology Society. Annual Conference, 2009 2009, pp. 463–466.
[23] R.N. Gursoy, O. Cevik, Design, characterization and in vitro evaluation of SMEDDS containing an anticancer peptide, linear LyP-1, Pharm. Dev. Technol. 19 (2014) 486–490.
[24] W. Li, J. Peng, L. Tan, J. Wu, K. Shi, Y. Qu, X. Wei, Z. Qian, Mild photothermal therapy/photodynamic therapy/chemotherapy of breast cancer by Lyp-1 modified Docetaxel/IR820 Co-loaded micelles, Biomaterials 106 (2016) 119–133.
[25] Z. Wang, Y. Yu, J. Ma, H. Zhang, H. Zhang, X. Wang, J. Wang, X. Zhang, Q. Zhang, LyP-1 modification to enhance delivery of artemisinin or fluorescent probe loaded polymeric micelles to highly metastatic tumor and its lymphatics, Mol. Pharm. 9 (2012) 2646–2657.
[26] X. Yu, A. Li, C. Zhao, K. Yang, X. Chen, W. Li, Ultrasmall semimetal nanoparticles of bismuth for dual-modal computed tomography/photoacoustic imaging and synergistic thermoradiotherapy, ACS Nano 11 (2017) 3990–4001.
[27] C.W. Su, C.S. Yen, C.S. Chiang, C.H. Hsu, S.Y. Chen, Multistage continuous targeting with quantitatively controlled peptides on Chitosan-lipid nanoparticles with multicore-shell nanoarchitecture for enhanced orally administrated anticancer in vitro and in vivo, Macromol. Biosci. (2016).
[28] D. Miao, M. Jiang, Z. Liu, G. Gu, Q. Hu, T. Kang, Q. Song, L. Yao, W. Li, X. Gao, M. Sun, J. Chen, Co-administration of dual-targeting nanoparticles with penetration enhancement peptide for antiglioblastoma therapy, Mol. Pharm. 11 (2014) 90–101.
[29] M. Uchida, H. Kosuge, M. Terashima, D.A. Willits, L.O. Liepold, M.J. Young, M.V. McConnell, T. Douglas, Protein cage nanoparticles bearing the LyP-1 peptide for enhanced imaging of macrophage-rich vascular lesions, ACS Nano 5 (2011) 2493–2502.
[30] G. Luo, X. Yu, C. Jin, F. Yang, D. Fu, J. Long, J. Xu, C. Zhan, W. Lu, LyP-1-conjugated nanoparticles for targeting drug delivery to lymphatic metastatic tumors, Int. J. Pharm. 385 (2010) 150–156.
[31] P.P. Karmali, V.R. Kotamraju, M. Kastantin, M. Black, D. Missirlis, M. Tirrell, E. Ruoslahti, Targeting of albumin-embedded paclitaxel nanoparticles to tumors, Nanomed.: Nanotechnol., Biol., Med. 5 (2009) 73–82.
[32] G. von Maltzahn, Y. Ren, J.H. Park, D.H. Min, V.R. Kotamraju, J. Jayakumar, V. Fogal, M.J. Sailor, E. Ruoslahti, S.N. Bhatia, In vivo tumor cell targeting with "click" nanoparticles, Bioconjugate Chem. 19 (2008) 1570–1578.
[33] Y.J. Jiang, S.J. Liu, Y. Zhang, H.C. Li, H. He, J.T. Dai, T. Jiang, W.H. Ji, D.Y. Geng, A.A. Elzatahry, A. Alghamdi, D.L. Fu, Y.H. Deng, D.Y. Zhao, Magnetic mesoporous nanospheres anchored with LyP-1 as an efficient pancreatic cancer probe, Biomaterials 115 (2017) 9–18.
[34] R.N. Gursoy, S. Benita, Self-emulsifying drug delivery systems (SEDDS) for improved oral delivery of lipophilic drugs, Biomed. Pharmacother. 58 (2004) 173–182.
[35] C.W. Pouton, Formulation of self-emulsifying drug delivery systems, Adv. Drug Deliv. Rev. 25 (1997) 47–58.
[36] S. Gibaud, D. Attivi, Microemulsions for oral administration and their therapeutic applications, Expert Opinion Drug Delivery 9 (2012) 937–951.
[37] C.W. Pouton, Lipid formulations for oral administration of drugs: non-emulsifying, self-emulsifying and 'self-microemulsifying' drug delivery systems, Eur. J. Pharm. Sci. 11 (2000) S93–S98.
[38] C.W. Pouton, C.J. Porter, Formulation of lipid-based delivery systems for oral administration: materials, methods and strategies, Adv. Drug Deliv. Rev. 60 (2008) 625–637.
[39] J.C. Lopez-Montilla, P.E. Herrera-Morales, S. Pandey, D.O. Shah, Spontaneous emulsification: mechanisms, physicochemical aspects, modeling, and applications, J. Disper. Sci. Technol. 23 (2002) 219–268.
[40] C.A. Miller, Spontaneous emulsification produced by diffusion - a review, Colloids Surf. 29 (1988) 89–102.
[41] N. Shahidzadeh, D. Bonn, O. Aguerre-Chariol, J. Meunier, Spontaneous emulsification: relation to microemulsion phase behaviour, Colloid Surf. A 147 (1999) 375–380.
[42] M.J. Groves, Formulation of Proteins and Peptides, Pharmaceutical Biotechnology, 2006.
[43] W. Fagir, R.M. Hathout, O.A. Sammour, A.H. ElShafeey, Self-microemulsifying systems of Finasteride with enhanced oral bioavailability: multivariate statistical evaluation, characterization, spray-drying and in vivo studies in human volunteers, Nanomed.: Nanotechnol., Biol., Med. 10 (2015) 3373–3389.
[44] K.A. Nematallah, N.A. Ayoub, E. Abdelsattar, M.R. Meselhy, M.M. Elmazar, A.H. El-Khatib, M.W. Linscheid, R.M. Hathout, K. Godugu, A. Adel, S.A. Mousa, Polyphenols LC-MS2 profile of Ajwa date fruit (Phoenix dactylifera L.) and their microemulsion: Potential impact on hepatic fibrosis, J. Funct. Foods 49 (2018) 401–411.
[45] S. Kamboj, V. Rana, Quality-by-design based development of a self-micro-emulsifying drug delivery system to reduce the effect of food on Nelfinavir mesylate, Int. J. Pharm. 501 (2016) 311–325.
[46] G. Leonaviciute, A. Bernkop-Schnurch, Self-emulsifying drug delivery systems in oral (poly)peptide drug delivery, Expert Opinion Drug Delivery 12 (2015) 1703–1716.
[47] W.J. Trickler, A.A. Nagvekar, A.K. Dash, A novel nanoparticle formulation for sustained paclitaxel delivery, AAPS PharmSciTech 9 (2008) 486–493.
[48] J.T. Lo, B.H. Chen, T.M. Lee, J. Han, J.L. Li, Self-emulsifying O/W formulations of paclitaxel prepared from mixed nonionic surfactants, J. Pharm. Sci. 99 (2010) 2320–2332.
[49] S. Yang, R.N. Gursoy, G. Lambert, S. Benita, Enhanced oral absorption of paclitaxel in a novel self-microemulsifying drug delivery system with or without concomitant use of P-glycoprotein inhibitors, Pharm. Res. 21 (2004) 261–270.
[50] G.R. Valicherla, K.M. Dave, A.A. Syed, M. Riyazuddin, A.P. Gupta, A. Singh, Wahajuddin, K. Mitra, D. Datta, J.R. Gayen, Formulation optimization of Docetaxel loaded self-emulsifying drug delivery system to enhance bioavailability and anti-tumor activity, Sci. Rep. 6 (2016) 26895.
[51] D.H. Truong, T.H. Tran, T. Ramasamy, J.Y. Choi, H.H. Lee, C. Moon, H.G. Choi, C.S. Yong, J.O. Kim, Development of solid self-emulsifying formulation for improving the oral bioavailability of erlotinib, AAPS PharmSciTech 17 (2016) 466–473.
[52] P.P. Constantinides, Lipid microemulsions for improving drug dissolution and oral absorption: physical and biopharmaceutical aspects, Pharm. Res. 12 (1995) 1561–1572.
[53] C.J.H. Porter, W.N. Charman, Uptake of drugs into the intestinal lymphatics after oral administration, Adv. Drug Deliv. Rev. 25 (1997) 71–89.
[54] V. Fogal, L. Zhang, S. Krajewski, E. Ruoslahti, Mitochondrial/cell-surface protein p32/gC1qR as a molecular target in tumor cells and tumor stroma, Cancer Res. 68 (2008) 7210–7218.
[55] Á.M.C. David Sánchez-Martín, Valentina Fogal, Erkki Ruoslahti, Luis Álvarez-Vallina, The multicompartmental p32/gClqR as a new target for antibody-based tumor targeting strategies, J. Biol. Chem. 286 (2011) 5197–5203.
[56] F. Madani, S. Lindberg, U. Langel, S. Futaki, A. Graslund, Mechanisms of cellular uptake of cell-penetrating peptides, J. Biophys. 2011 (2011) 414729.
[57] E.E. Ghosn, A.A. Cassado, G.R. Govoni, T. Fukuhara, Y. Yang, D.M. Monack, K.R. Bortoluci, S.R. Almeida, L.A. Herzenberg, L.A. Herzenberg, Two physically, functionally, and developmentally distinct peritoneal macrophage subsets, Proc. Nat. Acad. Sci. United States Am. 107 (2010) 2568–2573.
[58] X.Y. Zhang, W.Y. Lu, Recent advances in lymphatic targeted drug delivery system for tumor metastasis, Cancer Biol. Med. 11 (2014) 247–254.
[59] A. Ali Khan, J. Mudassir, N. Mohtar, Y. Darwis, Advanced drug delivery to the lymphatic system: lipid-based nanoformulations, International J. Nanomed. 8 (2013) 2733–2744.
[60] Y. Xie, T.R. Bagby, M.S. Cohen, M.L. Forrest, Drug delivery to the lymphatic system: importance in future cancer diagnosis and therapies, Expert Opinion Drug Delivery 6 (2009) 785–792.
[61] P. Kau, G.M. Nagaraja, H.Y. Zheng, D. Gizachew, M. Galukande, S. Krishnan, A. Asea, A mouse model for triple-negative breast cancer tumor-initiating cells (TNBC-TICs) exhibits similar aggressive phenotype to the human disease, BMC cancer 12 (2012).
[62] K. Tao, M. Fang, J. Alroy, G.G. Sahagian, Imagable 4T1 model for the study of late stage breast cancer, BMC cancer 8 (2008).
[63] L. Alberici, L. Roth, K.N. Sugahara, L. Agemy, V.R. Kotamraju, T. Teesalu, C. Bordignon, C. Traversari, G.P. Rizzardi, E. Ruoslahti, De novo design of a tumor-penetrating peptide, Cancer Res. 73 (2013) 804–812.
[64] P.V. Turner, C. Pekow, M.A. Vasbinder, T. Brabb, Administration of substances to laboratory animals: equipment considerations, vehicle selection, and solute preparation, J. Am. Assoc. Lab. Anim. Sci. 50 (2011) 614–627.
[65] L. Agemy, V.R. Kotamraju, D. Friedmann-Morvinski, S. Sharma, K.N. Sugahara, E. Ruoslahti, Proapoptotic peptide-mediated cancer therapy targeted to cell surface p32, Mol. Ther.: J. Am. Soc. Gene Ther. 21 (2013) 2195–2204.